PAPER • **OPEN ACCESS**

Experimental assessment of cracked tubular joints repaired with crack-deflecting holes and weld-toe grinding

To cite this article: S Riise *et al* 2023 *IOP Conf. Ser.: Mater. Sci. Eng.* **1294** 012032

Experimental assessment of cracked tubular joints repaired with crack-deflecting holes and weld-toe grinding

S Riise, M Atteya, O Mikkelsen and G Ersdal *

Faculty of Science and Technology, University of Stavanger, Norway

* Corresponding author: gerhard.ersdal@uis.no

Abstract. Tubular joints in offshore structures for energy production are exposed to cyclic loading and may experience fatigue cracking. Presently, the inspection method commonly used for such structures will primarily detect whether a member is flooded, which is an indication of through thickness cracks. As a result, repair methods suitable for repairing through thickness cracks that are cost-effective and quick to implement are needed. One such repair method could be crack arrest by hole drilling. However, the validity of such a repair method is at present not sufficiently proven. Hence, this paper presents the results of an experimental fatigue test of pre-cracked tubular joint repaired with crack-deflecting holes combined weld-toe grinding. One tubular double T joint was tested and underwent three-phases comprising of a pre-cracking phase, a repair phase and a post-repair testing phase. The through-thickness fatigue crack was achieved by subjecting the intact test joint to cyclic axial loading within the high-cycle fatigue domain. In the repair phase, crack-deflecting holes were drilled in front of each crack tip to arrest the crack ends. In addition, the weld-toe behind these holes were grinded to enhance the fatigue life of the repaired joint. The performances of the repaired test joint were then investigated in the last phase by subjecting it to further cyclic loading within the high cycles fatigue domain. In the test, the crack was successfully arrested in the crack-deflecting holes. Furthermore, the repair method indicated an apparent enhancement of the fatigue endurance of the cracked tubular joint when subjected to stress ranges within the high-cycle fatigue domain.

1. Introduction

Offshore jacket structures fabricated from steel tubular are widely used as offshore substructures for oil and gas exploration and are also increasingly used as substructures for offshore wind turbine. Figure 1, shows a typical offshore jacket structure. These fixed structures are exposed to a harsh environment with considerable cyclic wind and wave loadings in a corrosive environment, which can lead to fatigue cracking. Consequently, fatigue is one of the critical design criteria for such structures [1-4].

Although every effort is made in the design stage to avoid fatigue cracking in the offshore structures' service life, this may not be achieved. In addition, numerous offshore installations are ageing and have already passed their design life. Therefore, adequate inspection and repair are vital to maintain safe operating conditions and safely extend the life of the existing offshore structures. In most cases, the repair is difficult and expensive and may result in significant downtime with consequential loss [5].

Figure 1. Heimdal platform, typical offshore jacket structure (photo by Simen Riise)

An extensive number of repair methods exist, spanning from weld repair to mechanical fixing or removal and replacement of structural elements [6]. A similarity among these techniques is the necessity for heavy equipment, extensive planning, and substantial resource allocation, all of which contribute to high expenditure. Hence, there is a lack of economically temporary repair methods for tubular joints subjected to fatigue cracks. A well-known temporary repair method for plated structures subjected to fatigue cracks is crack tip holes and crack deflecting holes [7]. This method has been used with success in aeronautical industries and bridge engineering. It comprises drilling a through-thickness hole in the crack tip or crack tip proximity to arrest the crack in the hole, thereby reducing the stress intensity at the crack tip. Another cost-effective repair method proven to increase fatigue life is weld toe grinding [5], which implies profiling the weld toe to reduce the notch stress. The advantage of both these methods is that they do not require heavy equipment and are relatively easy to perform, which means lower costs.

The objective of the present investigation was to assess the effect of repairing a cracked tubular joint with crack-deflecting holes in combination with weld toe grinding, where the crack has been formed under high cycle fatigue conditions.

2. Specimen construction and fatigue test method

2.1. Specimen design

The joint design and fabrication are equal to the specimen tested by [8], thus enabling a comparison of the results. One DT-joint specimen was fabricated with the geometry shown in Figure 2.

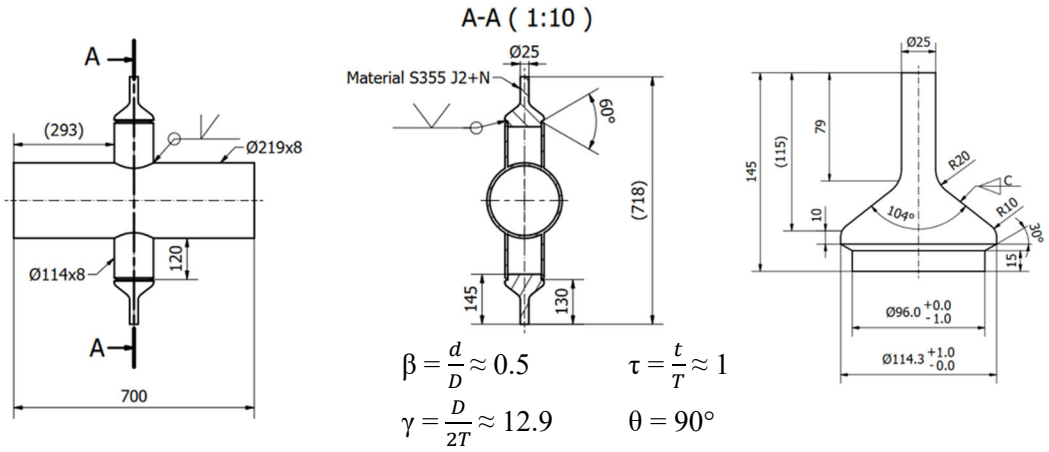

Figure 2. DT-joint Geometry [8]

NDT testing was conducted in compliance with the requirements stipulated in DNV-OS-C401, including 100% visual inspection, 100% magnetic particle testing and 100% ultrasonic testing. No weld improvement techniques were applied before the pre-cracking of the specimen. A picture of the DT-joint as fabrication and installed in the fatigue testing rig is shown in Figure 3.

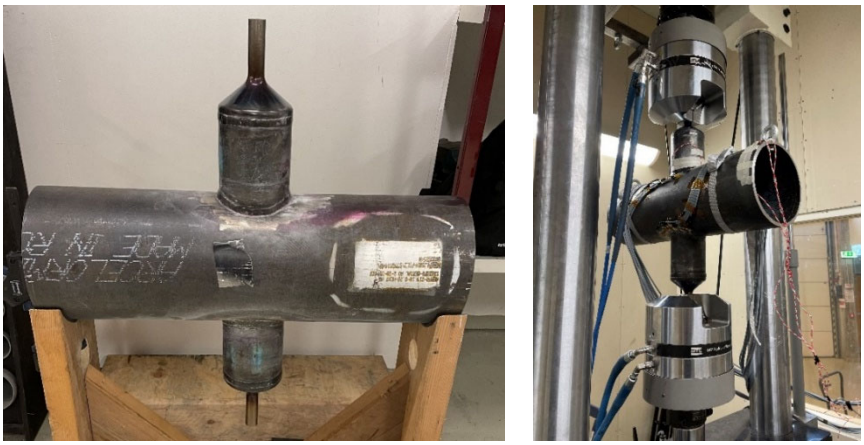

Figure 3. Specimen as-fabricated and installed in fatigue rig, respectively

2.2. Materials

The brace and chord were both made of hot-rolled, seamless pipes formed from normalised structural steel satisfying the grade requirements S355 G15+N. The cones were machined from a 120mm shaft of steel S355 J2+N.

A total of eight tensile tests was performed of the steel used in the fatigue test. The specimens were constructed according to ASTM A370 [9]. Four 3/4" specimens were cut out from the brace pipe and four 1" specimens were cut out from the chord pipe. The stress strain curve for one representative specimen is shown in Figure 4. This specimen had a tensile stress at yield of 423MPa (with a mean value for all tests at 406.5MPa) and an ultimate tensile stress of 544MPa (with a mean value for all tests at 528MPa).

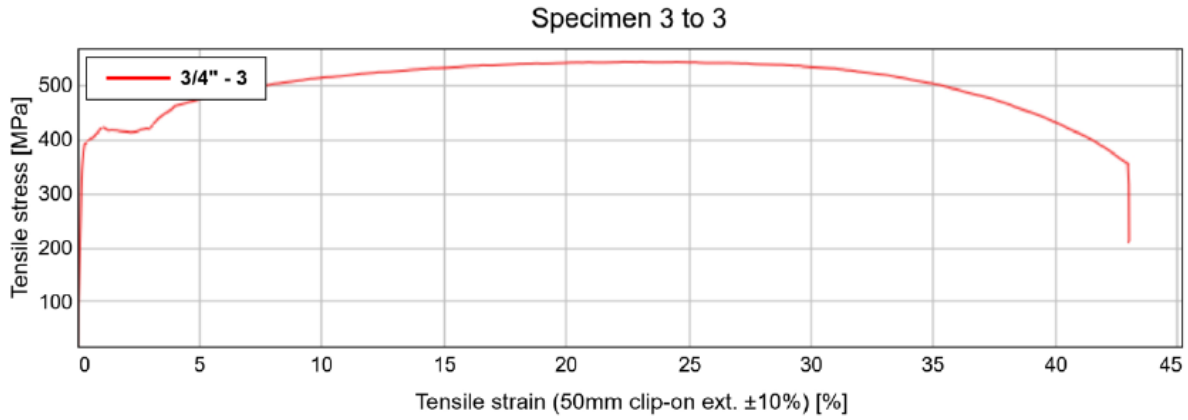

Figure 4. Stress strain curve for the steel applied in the tests.

2.3. Instrumentation

Linear electric strain gauges with grid lengths of 3mm and a nominal resistance of 120 were installed at critical locations on the DT joint to measure the stress distribution in the chord, detect and map crack propagation, and acquire the stress concentration factors. As the strain gauges are sensitive to temperature, thermocouples PT100 were glued to the specimen to constantly measure the temperature of the specimen and correct the strain readings.

In each quadrant of the specimen, six strain gauges were attached. The strain gauge layout within a single quadrant is depicted in Figure 5, featuring two SGs at the saddle point to capture the maximum hot spot stress with the aid of the linear extrapolation method described in DNV-RP-C203 [10]. The first row of strain gauges nearest to the weld toe were placed in extrapolation point A, as specified in DNV-RP-C203. Meanwhile, the strain gauges farthest from the weld toe, located at the saddle position, were positioned at extrapolation point B.

- Point A at chord surface normal to the weld toe = $0.2\sqrt{rt} = 4.4mm$
- Point B at chord surface normal to the weld toe = $2\pi R\,\frac{5}{360} = 9.6mm$

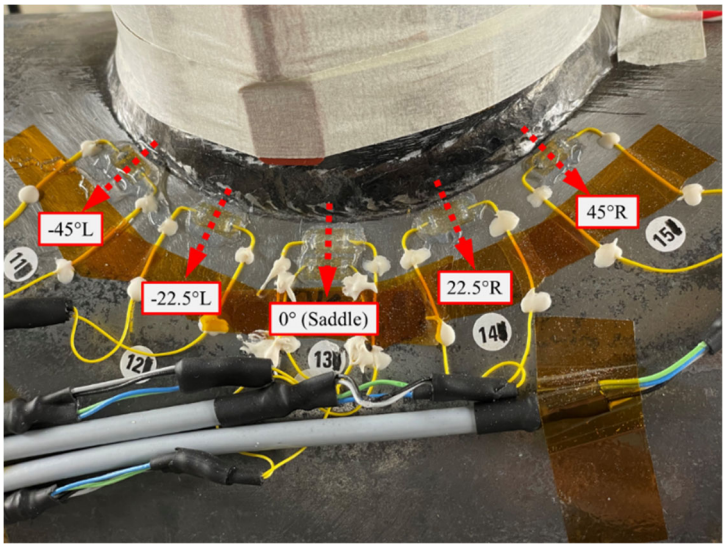

Figure 5. Strain gauge layout at quadrant 1

2.4. Fatigue testing condition

The specimen was tested under constant amplitude sinusoidal loading, in which sole axial force was applied through the brace. The entire fatigue testing process was carried out under load control, maintaining a positive R-ratio and a constant frequency between 3 to 10 Hz in air at room temperature. Before initiating the fatigue test, several preparatory steps were performed to ensure reliable results. Among these, the clamping stresses were recorded, and the reading frequency of the strain gauges was determined through a convergence study to ensure all peaks and valleys were captured during testing. The clamping stresses were decided to not be included in the testing and the strain gauge reading frequency was set to 300 Hz.

3. Result of fatigue test

3.1. Overview

The complete fatigue testing scheme of the DT joint aimed to evaluate the fatigue endurance of a cracked DT joint repaired with crack deflecting holes combined with weld toe grinding when degraded under high cycle fatigue conditions. To investigate this, one tubular DT-joint was tested through a three-phased testing scheme comprising:

1. **Pre-cracking:** the specimen was subjected to cyclic tension load under HCF conditions until a through-thickness crack was achieved.
2. **Repair:** two repair methods were performed on the specimen: weld toe grinding at the cracked quadrant and crack deflection holes at the crack tip proximity.
3. **Post-repair testing:** the repaired specimen was subjected to further cyclic loading under HCF conditions to evaluate the performance of the repair method. As a clear, indication of increased fatigue endurance was achieved the load was then significantly increased to break the specimen.

3.2. Pre-cracking phase

3.2.1. Stress Distribution. The stress distribution in the intact specimen was recorded as the pre-crack testing commenced and as expected for DT joints subjected to axial load the highest strain range was found in the saddle position. Furthermore, it can be seen in Figure 6 that the stress range is gradually decreasing towards the crown. It is also apparent in Figure 6 that stress ranges in all four quadrants are quite similar and symmetric around the saddle. This indicates symmetrically placed strain gauges and a lower probability of significant eccentricities in the specimen or test setup.

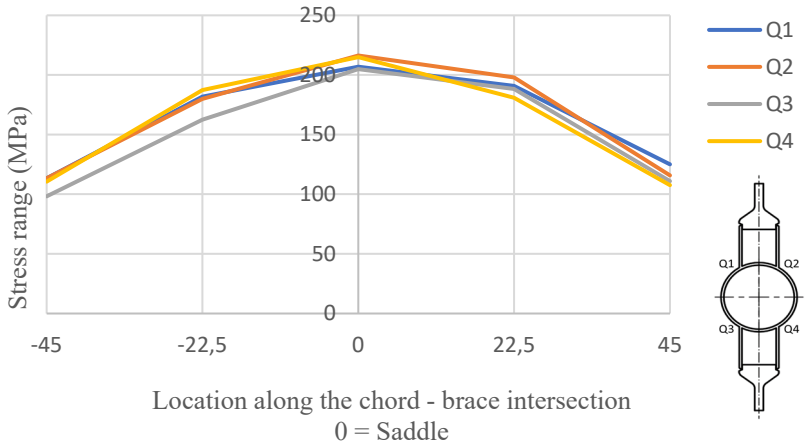

Figure 6. Stress range distribution at strain gauge closest to weld along chord-brace intersection ($\Delta P = 40$ kN)

3.2.2. SCF Calculation. In the pre-cracking phase, the stress concentration factors in the four saddle positions in the intact specimen were calculated based on the recorded HSS. The maximum SCF recorded under an axial load range of 40 kN was 20.45 located in Q2 and the average SCF of the four saddle positions was 19.89. Figure 7 below shows the SCF in the four quadrants. Furthermore, it shows the measured location of the strain gauges at a perpendicular distance from the weld toe along the chord surface and the ideal SG location when using linear extrapolation according to DNV is marked with the red dashed lines. Note that the SG positioned in saddle-b (in Figure 7) at Q3 was not measured after installation. Hence, the average SG placement in saddle-b from the other three quadrants is plotted.

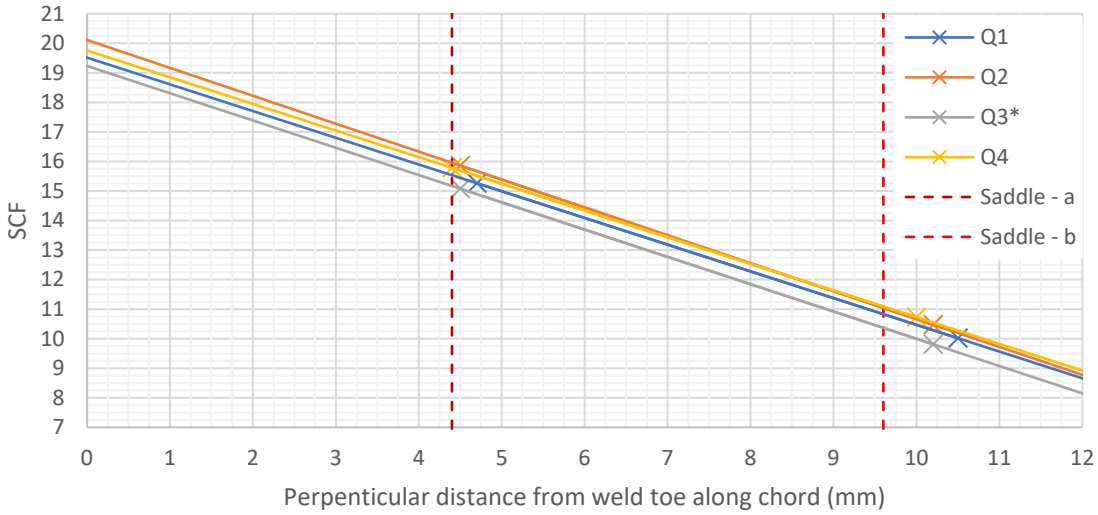

Figure 7. SCF at the four quadrants from the experimental work, with ΔP = 40 kN.
*The SG positioned in saddle-b at Q3 was not measured after installation. Hence, the average SG placement in saddle-b from the other three quadrants is plotted.

3.2.3. Pre cracking test loading. The load range and R-ratio maintained throughout the pre-cracking stage were 40kN and 0.1, respectively. Initially, the frequency was set to 6Hz but reduced to 3Hz after an 11% loss in the hot spot stress range at saddle point in Q3 at 300k cycles to ensure documentation of critical events. The maximum load reach in the testing (Pmax) was 45kN, while the minimum (Pmin) was 5kN. Stress distribution along the brace chord intersection and hot spot stresses at saddle positions were recorded. HSS recordings and load cell readings facilitated the calculation of SCFs.

3.2.4. Result of pre-cracking. The objective in the pre-cracking phase was to achieve a through-thickness crack, which could be observed with a 100% loss in hot spot strain readings. It was decided to stop the test at 1.515 million cycles as the strain gauges at the saddle and -22.5˚ degrees in Q3 had passed 90% and 96% drop in strain range, respectively. Hence, it was assumed that a through-thickness crack was achieved between the two strain gauges marking N3. The surface crack length was measured to 73mm, spanning between strain gauges at -45˚ to the strain gauge at +22.5˚. Based on the strain readings the remaining three quadrants seemed to not have undergone any significant damage. A summary of the fatigue life in Q3 is shown in Table 1.

Table 1. Fatigue testing results of the pre-cracking stage

Fatigue life	Number of cycles	Remark
N1	342 000	15% drop in the measured hot-spot strain*
N2	410 000	7.5mm surface crack length
N3	1 515 000	observation of 100% loss in the hot-spot strain readings**

*The hot-spot strain is measured by linear extrapolation from two strain gauges placed perpendicular to the weld toe.
**Two strain gauges lost over 90% of the strain range. Therefore, 100% strain range loss between these strain gauges is assumed.

3.3. Repair of the cracked DT-joint

3.3.1. Locating the crack tip. For crack-deflecting holes to increase fatigue endurance, it is vital to determine the exact location of the crack tips to place the holes in a favourable spot. Several steps were carefully carried out to validate the crack tip's location. First, the crack tips were located with the strain gauge readings and a microscope. Then MPI with fluorescent was conducted to validate the position. Finally, MPI with fluorescent was performed repeatedly with the specimen subjected to a static tensile load of 30kN to open the crack. As there was a good agreement on the crack tip position in all three inspections, the crack tip position was concluded to span from -38˚ to +21˚ in Q3.

3.3.2. Hole drilling and weld toe grinding. The specimen was repaired by drilling 18mm holes in the crack tip proximity. Positioning of the holes was made in alignment with Atteya [8], by centring the holes 12˚ ahead of the crack tip and shifting them 15mm perpendicular from the weld toe. As the crack spanned from -38˚ to +21˚, the holes were placed centred at -50˚ and +33˚. The objective of the crack-deflecting holes was to deflect the crack away from the weld toe, which holds significant stresses and arrests the crack in the holes.

In addition to the crack deflecting hole repair, weld toe grinding was performed in Q3 behind the holes. The repair was performed with a rotating "balled-nosed tree" carbide burr with a maximum diameter of 8mm and was used to grind the weld toe in compliance with BS 7608 [11]. The weld toe was further enhanced by sanding the weld toe in a direction perpendicular to the weld toe with a 240-grit paper, which produced a surface roughness of 58.5μm [12]. Post repair, the emerged weld toe profile exhibited an average depth and radius of 0.5mm and 3.4mm, respectively, which aligns with the DNV C203 and BS 7608 specifications.

3.3.3. Instrumentation in the repaired quadrant. After the repair, a set of three new strain gauges was installed around each crack deflecting hole in the repaired quadrant to monitor existing and new crack development. The strain gauge layout in Q3 is shown in Figure 8.

3.4. Performance of the repaired DT

3.4.1. Post-repair test Loading. In the final phase of the testing program, the performance of the repaired DT-Joint was tested by subjecting the specimen to additional cyclic stress. As the crack induces greater SCF while propagating, the load range was reduced to ensure that the stress range remained within the bounds of high cycle fatigue throughout the entire post-repair testing. A load range of 27kN was selected, maintaining an R-ratio of 0.1, resulting in a minimum load (Pmin) of 3kN and a maximum load (Pmax) of 30kN. The frequency was initially set at 5Hz but was later increased to 10Hz once the strain measurements stabilised and showed no indication of further crack propagation or initiation. The strain gauge readings stabilised after achieving a through-thickness crack between the crack-deflecting holes.

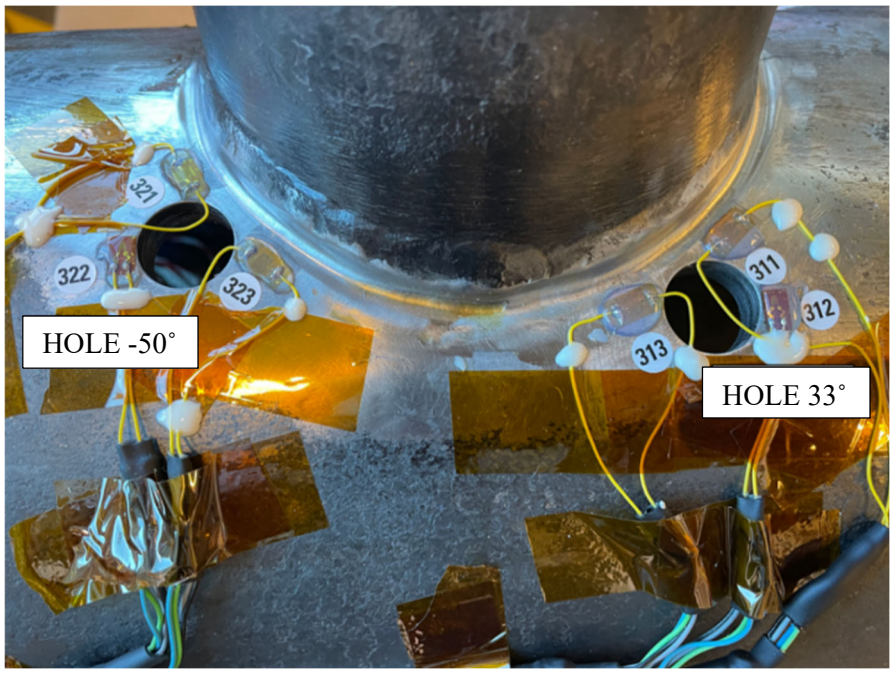

Figure 8. Strain gauge layout in repaired quadrant

3.5. *Result of post-repair testing.* A full through-thickness crack was achieved between the holes after 930 000 cycles, and the testing continued for another 2 585 000 cycles before test termination giving a total of 3 515 000 cycles in the post-repair testing. A summary of the fatigue life in the post-repair testing is shown in Table 2.

Table 2. Repaired specimen fatigue life

Fatigue Life	÷50˚ Hole	+33˚ Hole
Ni1	540 000	900 000
Ni2	910 000	930 000
Run out	3 515 000	

Ni1 surface crack into the hole; Ni2 though-thickness crack into the hole

3.6. Discussion

As there was no sign of crack initiation or further crack development, the conclusion that the repair had successfully increased the fatigue endurance in the specimen was drawn. Thus, the testing was stopped after a total of 3 515 000 cycles in the post-repair testing phase. However, to study further crack initiation and propagation it was decided to break the specimen by continuing the test at a significantly higher load range. The new load range chosen gave stresses in the borderline between High and low cycle fatigue.

3.7. Braking specimen load

3.7.1. Test loading when breaking the specimen. The new load range selected was adjusted to 54 kN, maintaining an R-ratio of 0.1. This load range gave a maximum load (Pmax) of 60 kN and a minimum load (Pmin) of 6 kN. Since the new stress range fell into the low cycle fatigue regime, events were anticipated to occur at a considerably accelerated rate. Hence the frequency was reduced back to 3 Hz.

3.7.2. Results from breaking the specimen. Previous testing of equal specimens has shown reverse coalescence, a phenomenon where the crack initiates in the weld toe beyond the crack-deflecting hole (crown side) and propagates back into the hole [8]. This behaviour does not align with the expected behaviour before the work of Atteya [8], where the crack initiates at the hole.

As per Atteya's discovery, the reverse coalescence phenomenon was present at both the crack-deflecting holes in the specimen tested in this experimental investigation, as shown in Figure 9.

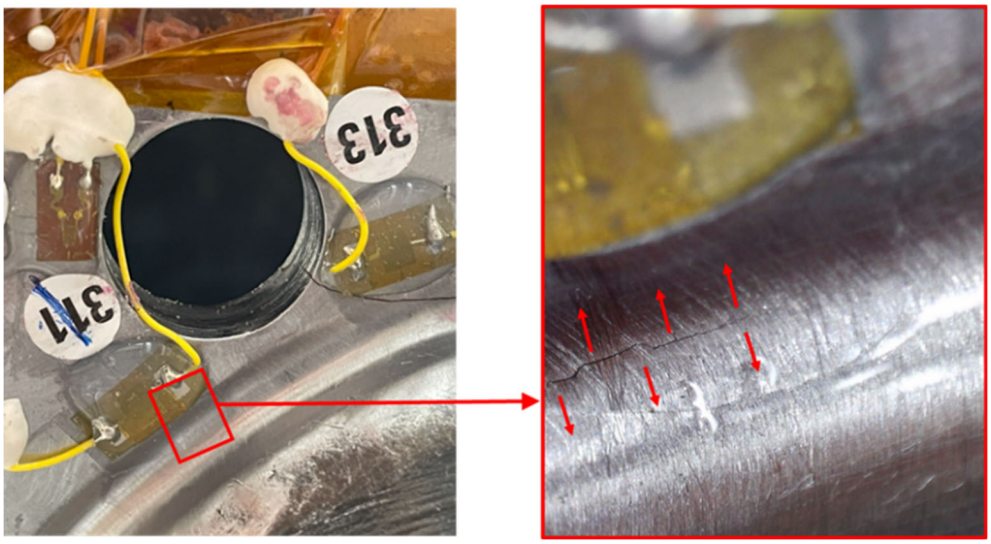

Figure 9. Crack initiation in front of SG crown-side at +33˚ hole

The testing was terminated after 260 000 cycles. At this point, the crack had propagated back into both holes and extended over a total length exceeding 1.5 multiplied by brace diameter marking N4. The fatigue life stages are summarized in Table 3.

Table 3. Fatigue life during breaking the specimen

Fatigue Life	÷50˚ Hole	+33˚ Hole
N1*	208 000	93 000
N2*	250 000	145 000
N4	260 000	

N1 Crack initiation beyond the hole 15% drop in strain range*
N2 Crack entering hole reversely*

4. Evaluation of the repair's effectiveness

4.1. Comparison with existing tests

An empirical approach to evaluating the efficacy of the repair is by comparing the number of cycles until N3 with those leading to N4. In this paper the ratio between N4 and N3 is defined as dR, Equation (1). From previous testing of similar tubular joints and test conditions without any repair the maximum recorded dR is about 30% [8, 13]. If the post repair fatigue test would reach a dR of 100% without any further crack initiation the repair would have fully reinstated the as-built fatigue life.

$$dR = \frac{N4 - N3}{N3}\% \quad (1)$$

The specimen was subjected to a lower cyclic stress range in the post-repair phase than in the pre-cracking phase. Therefore, a direct comparison to the pre-crack fatigue endurance would not be possible. Nevertheless, the cycle count to reach N3 under the post-repair stress range was estimated by shifting the SN curve to the N3 result from the pre-cracking phase, as shown in Figure 10. Subsequently, from this shifted S-N curve, the projected cycle count to achieve N3 under the stress range employed in the post-repair phase could be derived. Eventually, this enabled comparing the number of cycles in the post-repair phase and the estimated number of cycles to N3. The procedure employed to calculate dR is summarised as follows:

1. Pre-crack result ($\Delta P = 40\text{kN}$):
    a. $\sigma_{\text{nom}}(14.16\text{ MPa}) \cdot \text{SCF}(19.4) = \text{HSSr}(274.7\text{ MPa})$
    b. Number of cycles to N3 = 1 515 000
2. Shifting the SN curve to N3 from the pre-crack phase:
    a. New log(a) = 13.50
    b. m = 3
3. Estimate of the Number of cycles to N3 under post-repair load ($\Delta P = 27\text{kN}$):
    a. $\sigma_{\text{nom}}(9.19\text{ MPa}) \cdot \text{SCF}(19.4) = \text{HSSr}(178.24\text{ MPa})$
    b. Estimated number of cycles to N3 = $10^{\log(a) - m \cdot \log(\Delta\sigma)} = 5\,546\,000$
4. Number of cycles in the post-repair phase ($\Delta P = 27\text{kN}$):
    a. Number of cycles to run out = 3 515 000
5. Calculating dR = 3 515 000/ 5 546 000 = 63%

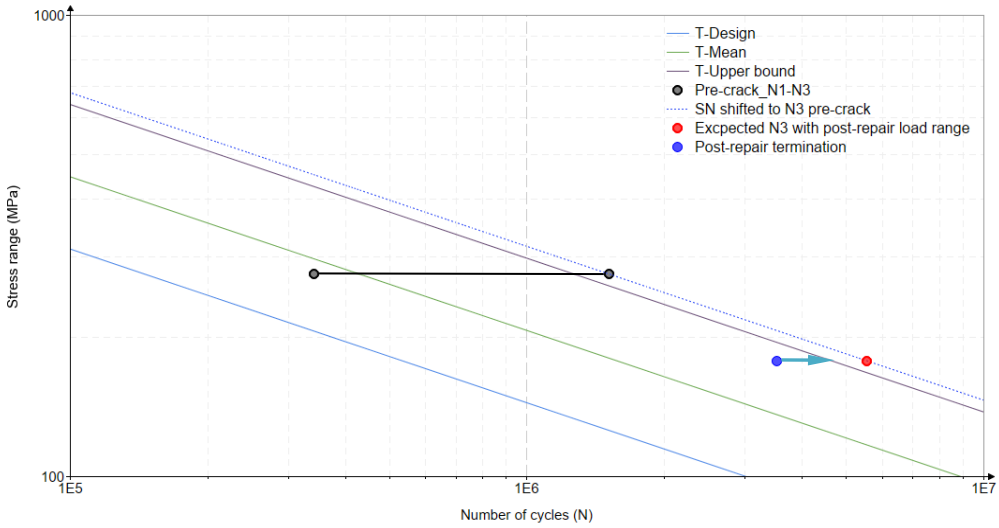

Figure 10. Standard SN curve and SN curve shifted to pre-crack result

The dR ratio of 63% derived from the approach employed in this section is about 100% higher than the greatest dR number for similar specimens tested without repair. Consequently, the conclusion can be drawn that drilling crack-deflecting holes combined with weld-toe grinding has successfully increased fatigue endurance. It should also be emphasised that N4 has not been reached under these loading conditions, but it was decided to stop the testing due to time limitations and that sufficient data

was achieved. Furthermore, there was no sign of crack initiation or development at the point of test termination. It should be emphasised that this approach is very conservative, as the post repair testing results is compared to a number of cycles laying above the upper bound of the SN curve.

4.2. Comparing recorded stress levels with SN-curve

4.2.1. Determining cycle count and stress range. In the post-repair testing, the specimen underwent 3 515 000 cycles until defined as a run-out. However, it took 930 000 cycles to achieve a through-thickness crack between the crack deflecting holes, in which the crown side strain gauge (SG with highest strain values) location where the new crack was expected to occur was subjected to a variable stress range as the crack propagated.

To evaluate the accumulated damage during these first 930 000 cycles and its relevance for the fatigue life of this location, an equivalent stress range for these cycles was calculated, and the resulting damage was established based on the SN curve. This damage was then used further to determine the equivalent number of cycles this part of the test represents, correcting for the stress level at this location after through thickness between the crack deflecting holes. The total number of cycles was then determined to 2 721 000.

The stress range recorded in post repair testing after a full through thickness crack between the holes was 250 MPa. However, only the directional strains are captured by the strain gauge therefore a finite element model was created to determine the factor to obtain the principal stresses [14]. Based on this analysis an amplification factor of 1.08 was determined which then gives a stress range of 269 MPa.

4.2.2. Comparison with SN curve

The basis for the comparison is 2.7 million cycles with a stress range of 269 MPa. Considering this result, it is immediately evident that the fatigue endurance in the post-repair testing is significantly higher than the upper bound of the T curve, which sets the basis for discussing the weld-toe grinding effect.

Both DNV-RP-C203 and BS 7608 provide an improved SN curve for welded connection subjected to weld toe grinding, as presented in Figure 11. By comparing the number of cycles from the design T curve with the improved SN curves, it is possible to derive an improvement factor of the weld toe grinding from DNV and BS for the given stress range of 269 MPa.

- Improved fatigue life according to DNV = 1.6
- Improved fatigue life according to BS = 2.0.

The reason for deriving these improvement factors, as opposed to simply extracting the number of cycles from the SN curves, is to enable the consideration of the fatigue endurance during the pre-cracking phase in the comparison. By utilising the SN curve shifted to the pre-crack result, the following number of cycles is expected:

- No improvement from weld-toe grinding: 1 616 000 cycles
- Improvement from grinding according to DNV: 2 636 000 cycles
- Improvement from grinding according to BS: 3 227 000 cycles
- **Number of cycles to run out in post-repair testing: 2 721 000 cycles**

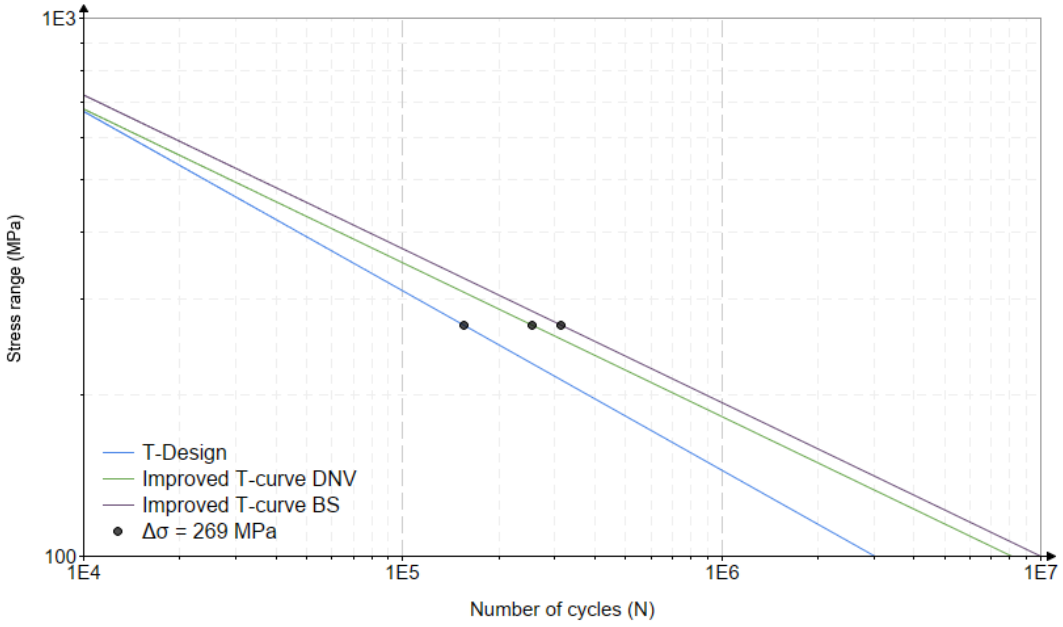

Figure 11. Improved SN curve from weld-toe grinding

It is evident from these considerations that the weld-toe grinding successfully increased the specimen's fatigue endurance. The number of cycles in the first attempt of the post-repair testing excided the number of cycles expected according to DNV when improved with weld toe grinding.

5. Conclusion

The performance of crack deflection holes as a repair method in the high-cycle fatigue domain has been investigated in this work, where crack deflection holes has been drilled on the chord-side in the vicinity of the crack tip. In addition, weld toe improve by grinding have been implemented.

Based on this work it is indicated that crack deflection holes combined with the weld-toe grinding managed to arrest the crack initiation in post-repair testing for high cycle fatigue loading. This is assumed to be a result of the weld-toe profile improvement, the improved surface roughness from the grinding, the sanding at the weld-toe and the reduced stress concentration due to the holes compared to an unrepaired cracked tubular joint.

The load range was increased in a second post-repair test to a high-stress range, leading to plastic strain and stress amplitudes and subsequent crack initiation and failure. In this high-stress range test, the weld toe-grinding had a limited enhancement on the specimen's fatigue life under such strain amplitudes.

Given the considerable variation and substantial uncertainties associated with the fatigue phenomenon, a single test cannot definitively establish a general understanding of the fatigue performance. However, in light of existing testing and the findings within this work, the effect of the studied repair method appears very promising.

6. Further work

As the experimental results indicated a significant fatigue life enhancement of tubular joints repaired with crack-deflection holes combined with weld-toe grinding, future research should focus on providing more empirical evidence on the method by investigating the effects of the repair on:

- Different joint configurations, e.g. T-joints, K-joints, and Y- joints
- Joints with different diameter and wall thickness ratios
- Joints subjected to different cyclic loading modes, e.g. In-plane and out-of-plane bending
- Joints in seawater with cathodic protection and free corrosion

Considering the crack initiation beyond the holes and the reverse coalescence phenomenon in the post-repair testing, future work should also focus on optimizing the cut-out repair, as already stated by Atteya [8]. An optimal hole shape, size and placement would decrease the stress concentration even further, making the repair method efficient for tubular joints subjected to higher nominal stress ranges and more extensive degradation.

Acknowledgement: The opinions expressed herein are those of the authors and they should not be construed as reflecting the views of any organization associated with the author.

References

[1] Almar-Næss A 1985 Fatigue handbook : offshore steel structures. 1985, Trondheim: Tapir.
[2] Atteya, M et al. 2021 Experimental and numerical study of the elastic SCF of tubular joints. *Mater.* **14**(15), 4220.
[3] Ersdal, G., J.V. Sharp, and A. Stacey, *Ageing and Life Extension of Offshore Structures: The Challenge of Managing Structural Integrity*. 2019, Newark: Newark: John Wiley & Sons, Incorporated.
[4] Lotsberg I 2016 *Fatigue Design of Marine Structures*. Cambridge: Cambridge: Cambridge University Press.
[5] Tubby P 1989 *OTH 89 370 Fatigue performance of repaired tubular joints*.
[6] Sharp J V and G Ersdal 2021 *Underwater inspection and repair for offshore structures*, Hoboken: John Wiley & Sons, Inc.
[7] Atteya M et al. 2020 *Crack arresting with crack deflecting holes in steel plates*. in *ASME 2020 39th Int. Conf. Ocean, Offshore Arctic Eng.***3,** https://doi.org/10.1115/OMAE2020-19358
[8] Atteya, M., 2023 Crack arresting using cutout repair in tubular offshore joints, *PhD thesis,* University of Stavanger (to be published), Norway.
[9] ASTM, *A370 − 19 Edition September 2019*. 2019, ASTM INTERNATIONAL.
[10] DNV, *DNV-RP-C203 - Fatigue design of offshore steel structures*. 2019, DNV AS.
[11] British Standard, *BS 7608:2014+A1:2015 - Guide to fatigue design and assessment of steel products*. 2015, BSI Standards Publication.
[12] Upmold. *Surface finish sandpaper grit chart*. 2017; Available from: https://upmold.com/surface-finish-sandpaper-grit-chart/.
[13] HSE, *OTH 92390 Background to new fatigue design guidance for steel joints and connections in offshore structures*. 1999.
[14] Riise S 2023 Experimental assessment of cracked tubular joints, *Master thesis,* University of Stavanger, Norway.